Design and Computational Analysis of 2-Chlorobenzoylated Quercetin Derivatives as Inhibitors of Estrogen Receptor Alpha

Dwi Utami[1*], Muhammad Fauzi[1,2], Laela Hayu Nurani[1], Any Guntarti[1], Citra Ariani Edityaningrum[1], Sugiyanto Sugiyanto[1], Lalu Muhammad Irham[1], Mustofa Ahda[1], Fara Azzahra[1,3], and Arif Budi Setianto[1]

[1]*Faculty of Pharmacy, Universitas Ahmad Dahlan, Jl. Prof. Dr. Soepomo, Janturan, Yogyakarta 55164, Indonesia*

[2]*Faculty of Pharmacy, Universitas Islam Kalimantan Muhammad Arsyad Al Banjari Banjarmasin, Jl. Adhyaksa, Banjarmasin 70122, Indonesia*

[3]*Diploma of Pharmacy, Akademi Farmasi Indonesia Yogyakarta, Jl. Veteran, Gg. Jambu, Pandeyan, Umbulharjo, Yogyakarta 55161, Indonesia*

* ***Corresponding author:***

email: dwi.utami@pharm.uad.ac.id

Received: September 26, 2025
Accepted: January 2, 2026

DOI: 10.22146/ijc.111483

Abstract: *Breast cancer remains a leading cause of mortality in women, highlighting the need for novel therapeutics. Quercetin, a natural flavonoid, shows anticancer potential but suffers from poor pharmacokinetics. To enhance its activity, 23 quercetin derivatives were designed as the flavonoid derivatives (FLD) series and evaluated using an integrated* in silico *workflow, including Lipinski's rule-of-five assessment, molecular docking against the estrogen receptor alpha (ERα; PDB ID: 3ERT), and ADMET prediction. Based on docking scores and favorable ADMET profiles, FLD-4, FLD-5, and FLD-6 were selected for 100 ns molecular dynamics simulations. FLD-4 exhibited the highest stability with an average RMSD of approximately 0.30 nm, while FLD-6 showed larger fluctuations (0.45 nm). SASA analysis revealed more compact structures for FLD-4 and the control ligand (131–133 nm^2) compared to quercetin and FLD-6. RMSF analysis confirmed reduced terminal residue flexibility for FLD-4 and FLD-5 (< 0.9 nm), whereas quercetin and FLD-6 fluctuated > 1.0 nm. MM-PBSA analysis further identified FLD-4 as the most stable complex (−205.409 ± 17.844 kJ/mol). Collectively, these results indicate that FLD-4 forms a stable, compact complex with improved binding affinity and drug-likeness, supporting its potential as a lead compound for flavonoid-based breast cancer therapy.*

Keywords: *quercetin derivatives; breast cancer; estrogen receptor alpha; molecular docking; ADMET; molecular dynamics; MM-PBSA*

INTRODUCTION

Breast cancer remains one of the most prevalent cancers worldwide and a leading cause of cancer-related mortality in women. Approximately 70% of breast cancers are hormone-dependent and express estrogen receptor alpha (ERα), making it a critical therapeutic target [1]. According to the latest GLOBOCAN 2022 data, an estimated 2.3 million new breast cancer cases and around 670,000 deaths were reported globally, with a continuous upward trend in many regions. In Indonesia, breast cancer is the most frequently diagnosed malignancy among women and contributes substantially to the national cancer burden, with an incidence rate of about 42.1 per 100,000 women and a mortality rate of 16.6 per 100,000. These epidemiological facts highlight the urgent need for more effective therapeutic candidates. In this context, flavonoid-based compounds, such as quercetin and its derivatives, have attracted increasing attention for their potential to modulate ERα activity and enhance therapeutic efficacy against hormone-dependent breast cancer [2-3].

Quercetin, a natural flavonoid abundant in fruits and vegetables, has been widely reported to exhibit

anticancer activity, including modulation of ERα signaling [4]. Nevertheless, its clinical utility is hindered by poor bioavailability, rapid metabolism, and limited binding affinity [5]. Structural modification of quercetin, particularly benzoylation with halogen-substituted aromatic groups, has emerged as a promising strategy to enhance hydrophobic interactions, improve stability, and increase receptor-binding potency [6]. The incorporation of a 2-chlorobenzoyl group into the quercetin scaffold is hypothesized to enhance binding interactions within the hydrophobic pocket of ERα, thereby improving its inhibitory potential. Unlike previous studies employing direct chlorination with Cl_2, this work introduces a 2-chlorobenzoyl substituent onto the quercetin core to enhance electronic effects and hydrophobic complementarity, representing a novel design approach [6-7]. Evidence from previous work on chlorinated quercetin derivatives supports that halogen substitution can modulate biological activity. Furthermore, recent studies demonstrate that structural modifications of flavonoids markedly affect their binding affinity and subtype-selectivity toward estrogen receptors, particularly through interactions with residues Glu353, Arg394, and His524 [8]. These findings suggest that rational substitution on the quercetin backbone, including halogenated benzoyl groups, may provide a promising strategy for optimizing ERα antagonists.

Screening of potent flavonoid derivatives can be performed using molecular docking to assess their binding affinity and interactions with the estrogen receptor. This initial computational approach provides valuable insights into potential activity and structural optimization of the compounds. Moreover, *in silico* methods offer significant advantages, including rapid execution, cost-effectiveness, and the ability to predict pharmacokinetic and toxicity profiles, thereby guiding further synthesis and experimental validation [9-10]. In this study, molecular docking was applied to predict the binding orientation and affinity of 2-chlorobenzoyl quercetin derivatives against ERα. Drug-likeness and pharmacokinetic properties were evaluated using Lipinski's Rule of Five and ADME predictions, while toxicity was assessed through *in silico* screening. Moreover, molecular dynamics (MD) simulations were conducted to explore the stability and conformational dynamics of the ligand–protein complexes over time. This integrated *in silico* workflow is expected to identify quercetin derivatives with improved ERα inhibitory potential, favorable pharmacokinetic profiles, and acceptable safety margins, thereby providing a rational basis for subsequent *in vitro* and *in vivo* investigations.

■ EXPERIMENTAL SECTION

Materials and Software

The primary material used in this study was quercetin (CID: 5280343), obtained from PubChem, which served as the parent ligand. The software employed included ChemDraw Ultra 20.0 and ChemDraw 3D for structural design and optimization, AutoDock 4.2 [11] for molecular docking, Discovery Studio Visualizer 202 and PyMOL [12] for visualization, SwissADME [13] and pkCSM for drug-likeness and ADMET prediction, as well as GROMACS [14] for MD simulations and MMP-BSA calculations. The target protein structure, ER-α, was retrieved from the Protein Data Bank (PDB ID: 3ERT) [15].

Procedure

Structure design and optimization

Quercetin consists of three main rings: ring A (chromone moiety), ring B (phenyl group attached at position C2), and ring C (heterocyclic pyrone ring connecting rings A and B). The hydroxyl groups at positions 3, 5, and 7 (ring A) and positions 3′ and 4′ (ring B) are key reactive sites for chemical modification. Quercetin was modified into 23 novel derivatives by substituting these hydroxyl groups with benzoyl substituents. The modifications were performed using ChemDraw Ultra 20.0, and the resulting structures were optimized in ChemDraw 3D employing the Merck Molecular Force Field 94 (MMFF94) method to obtain the most stable conformations. The optimized files were saved in .pdb format for subsequent docking studies. Fig. 1 illustrates the parent quercetin structure [16].

The synthetic pathway presented in Fig. 1 is a conceptual design derived from literature data and *in silico*

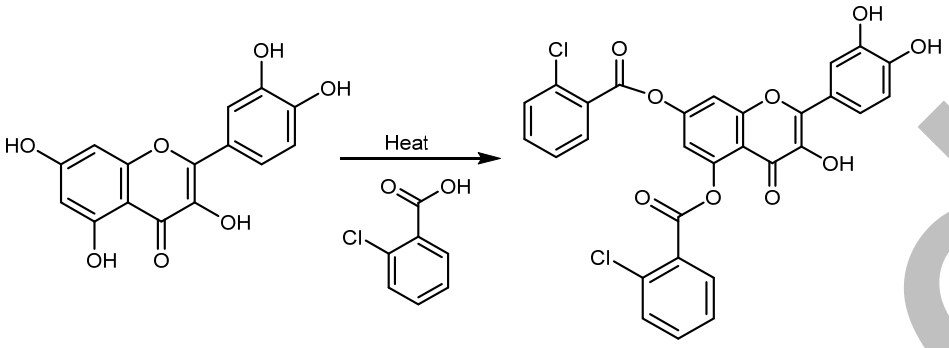

Fig 1. Synthesis of flavonoid derivatives

analysis, intended to illustrate the predicted mechanism of quercetin benzoylation with 2-chlorobenzoyl chloride. This schematic representation was developed to support the rational design of the proposed derivatives and to guide future experimental synthesis. No actual chemical synthesis or reaction optimization was performed in this study, as the current work focuses exclusively on computational modeling. The depiction of the reaction conditions, including the use of mild heating, is based on common benzoylation/acylation strategies for flavonoids reported in the literature [17-18] and therefore serves only as a theoretical framework for subsequent laboratory validation.

Protein preparation

The three-dimensional structure of ER-α was prepared using AutoDock Tools. The preparation process involved removing water molecules, adding polar hydrogen atoms, repairing missing residues, and defining the grid center based on the position of the co-crystallized ligand. The prepared protein structure was saved in .pdbqt format.

Drug-likeness and ADMET prediction

The drug-likeness of all quercetin derivatives was evaluated using SwissADME, focusing on key parameters of Lipinski's Rule of Five, including molecular weight, log P, and hydrogen bond donors and acceptors. Furthermore, ADMET profiling was performed using the pkCSM server to predict pharmacokinetic properties, including absorption, distribution, metabolism, and excretion, as well as potential toxicities [19].

Molecular docking

Molecular docking was conducted using AutoDock 4.2 with the Lamarckian Genetic Algorithm (LGA) to predict ligand–receptor interactions and binding affinities. The protein structure of hERα was prepared by removing water molecules and co-crystallized ligands, adding polar hydrogens, and assigning Gasteiger charges. All ligands were energy-minimized and protonated at physiological pH (7.4) [20].

Docking parameters were set as follows: 100 GA runs, population size of 150, maximum number of energy evaluations = 2.5×10^6, and RMSD tolerance for clustering = 2.0 Å. The grid box was defined based on the active site of the co-crystallized ligand, with a grid size of $40 \times 40 \times 40$ points and spacing of 0.375 Å, centered at coordinates (x = 30.01; y = −1.913; z = 24.207). The docking results were ranked by binding free energy (ΔG), and the top-ranked pose for each ligand was analyzed for hydrogen bonding and hydrophobic interactions using Discovery Studio Visualizer 2021.

Method validation

To validate the reliability of the docking procedure, a re-docking experiment was performed using the native ligand 4-hydroxytamoxifen. The ligand was extracted from the crystallographic structure of hERα and re-docked using the same parameters as above. The resulting docked pose closely overlapped with the crystallographic ligand, yielding an RMSD of 1.01 Å (Fig. 2) and a binding free energy (ΔG) of −11.40 kcal/mol, confirming the accuracy of the docking setup (RMSD < 2.0 Å is generally acceptable). Therefore, the validated parameters were applied for docking all FLD derivatives.

MD simulation

The quercetin derivative with the highest molecular docking binding affinity was further subjected to a 100 ns

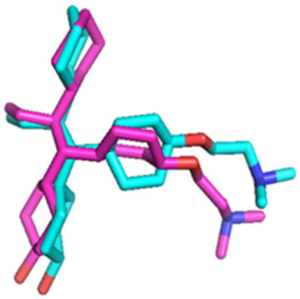

Fig 2. Overlay of the ligand position resulting from redocking 4-hydroxytamoxifen with the crystallographic results (Pink = crystallographic results and Blue = redocking pose)

MD simulation with a 2 fs timestep using GROMACS version 2016.3 and the AMBER99SB-ILDN force field. Ligand topology and parameters were generated using ACPYPE. Long-range electrostatic interactions were calculated using the Particle Mesh Ewald (PME) method, while the system was solvated in a TIP3P water box and neutralized with Na^+ and Cl^- ions. The simulation process included energy minimization, heating to 310 K, equilibration in the NVT and NPT ensembles, and production runs of 100 ns [20].

The structural stability and dynamic behavior of the protein–ligand complexes were analyzed using root mean square deviation (RMSD) to assess overall structural stability, root mean square fluctuation (RMSF) to evaluate the flexibility of amino acid residues in the binding site, and solvent accessible surface area (SASA) to determine solvent exposure of the protein surface. Furthermore, the binding free energy (ΔG_bind) was calculated using the Molecular Mechanics Poisson–Boltzmann Surface Area (MMP-BSA) method implemented in the g_mmpbsa package integrated with GROMACS. The binding free energy was obtained as the difference between the free energies of the complex and its individual components (receptor and ligand) using the equation ΔG_bind = G_complex – G_receptor– G_ligand [21].

The polar solvation energy was computed using the Poisson–Boltzmann equation with a solvent dielectric constant of 80, while the nonpolar contribution was estimated based on the SASA using a solvent radius of 1.4 Å. The total binding energy was calculated from 500 snapshots extracted from the 1–100 ns simulation trajectory. Replicate simulations were not performed, as the analysis focused on the most stable complex obtained from the initial docking results [12-13,22].

■ RESULTS AND DISCUSSION

Structural Design and Optimization of Compounds

Quercetin contains five hydroxyl groups distributed across ring A (positions 5 and 7), ring C (position 3), and ring B (positions 3′ and 4′). These hydroxyl groups are the primary targets for structural modification, as they play a crucial role in hydrogen bonding but also contribute to quercetin's poor solubility and limited bioavailability [14]. To address these limitations, structural modifications were performed by substituting the hydroxyl groups with chlorinated benzoyl substituents. The designed compounds were constructed in ChemDraw and subsequently subjected to geometric optimization in Chem3D using the MMFF94 method. The optimization results demonstrated that all 23 quercetin derivatives achieved the lowest and most stable energy conformations, as summarized in Table 1. Furthermore, the synthesized derivatives were abbreviated as FLD, representing flavonoid derivatives.

Table 1. Quercetin derivatives with Y = $–C_6H_5–C(=O)–Cl$

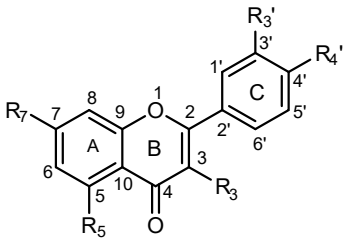

Compound	R3	R5	R7	R3'	R4'
Quercetin ($C_{15}H_{10}O_7$)	–OH	–OH	–OH	–OH	–OH
FLD-1 ($C_{29}H_{16}Cl_2O_9$)	–OH	–Y	–Y	–OH	–OH
FLD-2 ($C_{43}H_{22}Cl_4O_{11}$)	–Y	–Y	–Y	–OH	–Y
FLD-3 ($C_{36}H_{19}Cl_3O_{10}$)	–OH	–Y	–OH	–Y	–Y
FLD-4 ($C_{29}H_{16}Cl_2O_9$)	–OH	–OH	–OH	–Y	–Y

Compound	R3	R5	R7	R3'	R4'
FLD-5 ($C_{36}H_{19}Cl_3O_{10}$)	–OH	–OH	–OH	–Y	–Y
FLD-6 ($C_{50}H_{25}Cl_5O_{12}$)	–Y	–Y	–Y	–Y	–Y
FLD-7 ($C_{22}H_{13}ClO_8$)	–OH	–OH	–Y	–Y	–OH
FLD-8 ($C_{29}H_{16}Cl_2O_9$)	–Y	–Y	–Y	–OH	–OH
FLD-9 ($C_{36}H_{19}Cl_3O_{10}$)	–Y	–Y	–OH	–Y	–Y
FLD-10 ($C_{29}H_{16}Cl_2O_9$)	–OH	–Y	–OH	–Y	–OH
FLD-11 ($C_{22}H_{13}ClO_8$)	–OH	–Y	–OH	–OH	–OH
FLD-12 ($C_{29}H_{16}Cl_2O_9$)	–Y	–Y	–OH	–OH	–OH
FLD-13 ($C_{29}H_{16}Cl_2O_9$)	–OH	–Y	–OH	–OH	–Y
FLD-14 ($C_{36}H_{19}Cl_3O_{10}$)	–Y	–Y	–OH	–OH	–Y
FLD-15 ($C_{29}H_{16}Cl_2O_9$)	–Y	–OH	–OH	–OH	–Y
FLD-16 ($C_{36}H_{19}Cl_3O_{10}$)	–Y	–OH	–OH	–Y	–Y
FLD-17 ($C_{29}H_{16}Cl_2O_9$)	–OH	–OH	–OH	–OH	–Y
FLD-18 ($C_{22}H_{13}ClO_8$)	–OH	–OH	–Y	–OH	–Y
FLD-19 ($C_{29}H_{16}Cl_2O_9$)	–OH	–OH	–Y	–Y	–OH
FLD-20 ($C_{29}H_{16}Cl_2O_9$)	–OH	–OH	–Y	–Y	–Y
FLD-21 ($C_{29}H_{16}Cl_2O_9$)	–OH	–OH	–Y	–OH	–OH
FLD-22 ($C_{22}H_{13}ClO_8$)	–Y	–OH	–OH	–Y	–OH
FLD-23 ($C_{29}H_{16}Cl_2O_9$)	–OH	–OH	–OH	–Y	–OH

Lipinski's Rule of Five Analysis

A total of 23 designed derivatives of 2-chlorobenzoyl–quercetin, along with the parent compound quercetin, were systematically evaluated based on Lipinski's Rule of Five to determine their potential as orally active drug candidates [15]. The parameters analyzed included molecular weight (MW), partition coefficient (log P), hydrogen bond donors (HBD), and hydrogen bond acceptors (HBA) [16]. The results demonstrated that only the parent compound quercetin and one derivative, FLD-7, fully complied with Lipinski's criteria, suggesting favorable oral bioavailability. In contrast, most of the other derivatives exhibited at least one violation, predominantly due to molecular weight exceeding 500 Da and log P values greater than 5. These deviations may indicate potential limitations in solubility and membrane permeability. A detailed summary of these properties for each compound is presented in Table 2.

Table 2. Lipinski's rule of five results

Compound	MW (g/mol)	Log P	H Donor	H Acceptor	Formula	Conclusion
Quercetin	302.24	1.23	5	7	$C_{15}H_{10}O_7$	Complies
Tamoxifen	387.51	5.36	1	3	$C_{26}H_{29}NO_2$	Not Comply (Log P)
FLD-1	579.34	5.05	3	9	$C_{29}H_{16}Cl_2O_9$	Not Comply (MW and Log P)
FLD-2	856.44	8.82	1	11	$C_{43}H_{22}Cl_4O_{11}$	Not Comply (MW and Log P)
FLD-3	717.89	6.92	2	10	$C_{36}H_{19}Cl_3O_{10}$	Not Comply (MW and Log P)
FLD-4	579.34	5.16	3	9	$C_{29}H_{16}Cl_2O_9$	Not Comply (MW and Log P)
FLD-5	717.89	7.04	2	10	$C_{36}H_{19}Cl_3O_{10}$	Not Comply (MW and Log P)
FLD-6	994.99	10.56	0	12	$C_{50}H_{25}Cl_5O_{12}$	Not Comply (MW and Log P)
FLD-7	440.79	3.32	4	8	$C_{22}H_{13}ClO_8$	Complies
FLD-8	579.34	5.05	3	9	$C_{29}H_{16}Cl_2O_9$	Not Comply (MW and Log P)
FLD-9	717.89	6.84	2	10	$C_{36}H_{19}Cl_3O_{10}$	Not Comply (MW and Log P)
FLD-10	579.34	5.10	3	9	$C_{29}H_{16}Cl_2O_9$	Not Comply (MW and Log P)
FLD-11	440.79	3.19	4	8	$C_{22}H_{13}ClO_8$	Not Comply (MW and Log P)

Compound	MW (g/mol)	Log P	H Donor	H Acceptor	Formula	Conclusion
FLD-12	579.34	5.05	3	9	$C_{29}H_{16}Cl_2O_9$	Not Comply (MW and Log P)
FLD-13	579.34	5.08	3	9	$C_{29}H_{16}Cl_2O_9$	Not Comply (MW and Log P)
FLD-14	717.89	6.86	2	10	$C_{36}H_{19}Cl_3O_{10}$	Not Comply (MW and Log P)
FLD-15	579.34	5.11	3	9	$C_{29}H_{16}Cl_2O_9$	Not Comply (MW and Log P)
FLD-16	717.89	6.92	2	10	$C_{36}H_{19}Cl_3O_{10}$	Not Comply (MW and Log P)
FLD-17	579.34	5.16	3	9	$C_{29}H_{16}Cl_2O_9$	Not Comply (MW and Log P)
FLD-18	440.79	3.32	4	8	$C_{22}H_{13}ClO_8$	Complies
FLD-19	579.34	5.32	3	9	$C_{29}H_{16}Cl_2O_9$	Not Comply (MW and Log P)
FLD-20	579.34	5.31	3	9	$C_{29}H_{16}Cl_2O_9$	Not Comply (MW and Log P)
FLD-21	579.34	5.25	3	9	$C_{29}H_{16}Cl_2O_9$	Not Comply (MW and Log P)
FLD-22	440.79	3.17	4	8	$C_{22}H_{13}ClO_8$	Not Comply (MW and Log P)
FLD-23	579.34	5.09	3	9	$C_{29}H_{16}Cl_2O_9$	Not Comply (MW and Log P)

Molecular Docking Simulation

The re-docking of 4-hydroxytamoxifen successfully reproduced the experimental binding orientation within the active pocket of hERα (RMSD = 1.01 Å), confirming that the applied docking parameters were reliable for subsequent screening of quercetin and FLD derivatives. Further interaction analysis revealed that tamoxifen formed hydrogen bonds with Glu353 and Arg394, along with additional van der Waals, pi-alkyl, and pi-sulfur interactions that contributed to complex stability [23]. These residues are known to play an essential role in ligand binding to hERα. Therefore, the docking method employed in this study is valid and reliable for predicting interactions between quercetin derivatives and the estrogen receptor.

A total of 23 modified quercetin derivatives (FLD-1 to FLD-23) were successfully docked against the hERα receptor. The docking results showed variations in binding free energy (ΔG) and inhibition constant (Ki), which reflect the affinity of each compound for the receptor. The lower the ΔG and Ki values, the greater the ligand's affinity for the target receptor. The molecular docking results are shown in Table 3.

Molecular docking results indicated that several FLD derivatives exhibited significantly higher binding affinity to hERα compared to the parent quercetin and

Table 3. Binding free energy and inhibition constant ofFLD-1–FLD-23 against the hERα receptor

Compounds	Free Energy (ΔG, kcal/mol)	Inhibition Constant (Ki) (nM)	Type of Interaction	Amino Acid Residues
Quercetin	-7.50	3.18 uM	Hydrogen bond Hydrophobic interaction Electrostatic interaction	Glu353, Glu419 Leu525, Ile424, Gly521, Met388, Leu384, Arg394, Leu391, Phe404, Gly420, His524, Val418, Met343 Met421, Leu349 Leu387
Native ligand (Tamoxifen)	-11.40	867.83 pM	Hydrogen bond Hydrophobic interaction Electrostatic interaction	Arg394, Glu353 Leu428, Phe404, Met388, Gly521, His524, Gly420, Glu419, Leu384, Thr347, Trp383, Leu349 Leu387, Leu391, Ala350, Leu525, Met421
FLD-1	−12.72	477.96 pM	Hydrogen bond Hydrophobic interaction Electrostatic interaction	Met343, Thr347, Asp351 Phe404, Met388, Gly521, His524, Gly420, Glu419, Trp383, Arg394, Glu353 Met421, Leu525, Leu387, Leu349, Leu384, Leu391
FLD-2	−13.15	228.97 pM	Hydrogen bond Hydrophobic interaction Electrostatic interaction	Cys530 Arg394, Trp383, Leu391, Phe404, Leu384, Gly521, Gly420, Met528, Lys529, Val533, Leu539 Leu428, Ala350, Leu387, Leu349

Compounds	Free Energy (ΔG, kcal/mol)	Inhibition Constant (Ki) (nM)	Type of Interaction	Amino Acid Residues
FLD-3	−13.54	118.47 pM	Hydrogen bond Hydrophobic interaction Electrostatic interaction	Thr367 Leu536, Leu354, Met388, Trp383, Met528, Gly521, His524, Gly420, Glu419, Ile424, Leu349, Leu384, Phe404, Glu353, Arg394 Ala350, Leu525, Met421
FLD-4	−12.72	476.73 pM	Hydrophobic interaction Electrostatic interaction	Leu539, Met528, Thr347, His524, Gly420, Gly521, Glu419, Val418, Arg394, Phe404, Glu353, Leu349. Leu536 Ala350, Leu384, Met388, Ile424, Met421, Leu387
FLD-5	−13.61	104.87 pM	Hydrogen bond Hydrophobic interaction Electrostatic interaction	Asp351, Met343 Trp383, Thr347, Met528, Gly521, His524, Gly420, Glu419, Met388, Phe404, Arg394, Glu353 Leu525, Met421, Leu393, Leu349, Leu387, Leu384, Ala350
FLD-6	−12.69	501.71 pM	Hydrophobic interaction Electrostatic interaction Halogen interaction	Arg394, Trp383, Leu539, Leu354, Val533, Cys530, Met528, Gly521, Ile424, Leu428, Leu384, Phe404, Leu391 Leu349, Ala350, Leu536 Leu387
FLD-7	−8.98	260.42 nM	Hydrogen bond Hydrophobic interaction Electrostatic interaction	Met343, Thr347 Met528, Leu539, Leu536, Leu364, Met388, Trp383, Leu384, Leu387, Arg394, Phe404 Leu391, Leu349, Leu525, Ala350
FLD-8	−12.64	538.78 pM	Hydrogen bond Hydrophobic interaction Electrostatic interaction	Glu419, Val418, Gly420, Gly521, Ile424, Leu428, Phe404, Leu349, Trp383, Leu354, Leu539, Leu536, Lys529 His524, Leu384, Leu387, Leu391, Leu346, Ala340, Leu525, Met528
FLD-9	−12.63	556.75 pM	Hydrophobic interaction Electrostatic interaction	Leu539, Glu419, Gly420, His524, Gly521, Ile424, Leu428, Phe404, Leu391, Leu536 Met528, Leu525, Ala350, Leu346, Leu354, Leu384, Leu387, Val533
FLD-10	−11.09	7.48 nM	Hydrogen bond Hydrophobic interaction Electrostatic interaction	Glu419, Asp351 Leu349, Arg394, Thr347, His524, Val418, Gly420, Met421, Ile424, Leu428, Phe404 Leu391, Leu346, Met388, Leu387, Leu536, Leu354, Ala350, Leu384
FLD-11	−9.63	86.94 nM	Hydrogen bond Hydrophobic interaction Electrostatic interaction	Asp351, Glu419 Leu349, Trp383, Thr347, His524, Val418, Gly420, Leu428, Ile424 Leu391, Met388, Leu387, Ala350, Leu525, Leu384, Met421, Leu346
FLD-12	−10.09	40.24 nM	Hydrogen bond Hydrophobic interaction Electrostatic interaction	Asp351 Leu428, Gly521, Met388, Phe404, Arg394, Leu391, Trp383, Thr347, Met528, His524 Met421, Leu525, Leu384, Leu387, Ala350, Cys350
FLD-13	−11.10	7.32 nM	Hydrogen bond Hydrophobic interaction Electrostatic interaction	Glu419, Asp351 Thr347, Leu354, Val418, Gly420, Ile424, His524, Leu428, Phe404, Leu349, Glu353, Arg394, Leu384 Leu391, Met388, Leu387, Leu536, Leu525, Ala350, Met421, Leu346
FLD-14	−11.20	6.15 nM	Hydrogen bond	His534, Glu353

Compounds	Free Energy (ΔG, kcal/mol)	Inhibition Constant (Ki) (nM)	Type of Interaction	Amino Acid Residues
			Hydrophobic interaction Electrostatic interaction	Phe404, Gly521, Tyr526, Met528, Thr347, Leu349, Leu387, Arg394 Leu428, Ile424, Met388, Leu346, Ala350, Trp383, Leu525, Leu384
FLD-15	−11.45	4.05 nM	Hydrogen bond Hydrophobic interaction Electrostatic interaction	Glu353 Met388, Leu391, Leu384, His524, Gly521, Gly420, Met528, Asp351, Leu354, Thr347, Leu349, Arg394, Phe404 Leu387, Ala350, Leu346, Trp383, Leu536, Leu525
FLD-16	−12.43	773.63 pM	Hydrogen bond Hydrophobic interaction Electrostatic interaction	Asp351 Thr347, Lys529, Gly421, Ile428, His524, Glu419, Gly420, Met421, Leu384, Met388, Phe404, Arg394, Glu353, Leu349, Leu536 Leu354, Leu391
FLD-17	−9.10	213.11 nM	Hydrogen bond Hydrophobic interaction Electrostatic interaction	Asp351 Met528, Thr347, Met388, Leu384, Met421, Arg394, Glu353, Leu349, Phe404, Leu428, Trp383, Leu354 Ala350, Leu525, Leu391
FLD-18	−10.56	18.24 nM	Hydrogen bond Hydrophobic interaction Electrostatic interaction Halogen interaction	Met343 Met528, Thr347, Ile424, Leu428, Met388, Arg394, Phe404, Glu353 Leu384, Leu391, Leu346, Leu349, Leu536, Leu539 Leu387
FLD-19	−10.87	10.80 nM	Hydrogen bond Hydrophobic interaction Electrostatic interaction	Thr347, Met343 Leu391, Leu387, Trp383, Leu536, Leu539, Met528, Met388, Gly521, His524, Gly420, Glu419, Phe404, Leu391 Met421, Leu384, Ala350,
FLD-20	−10.81	11.95 nM	Hydrogen bond Hydrophobic interaction Electrostatic interaction	Leu387, Arg394 Leu384, Gly521, Met388, Phe404, Gly390, Glu353, Thr347 Ile424, Met421, Leu536, Leu391, Ala350, Leu354, Leu525
FLD-21	−9.81	64.40 nM	Hydrogen bond Hydrophobic interaction Electrostatic interaction	Glu419, His524, Asp351 Arg394, Thr347, Val418, Gly420, Trp383, Phe404, Leu384, Met388 Leu387, Ala350, Leu346, Leu525, Leu391, Leu349
FLD-22	−11.77	2.37 nM	Hydrogen bond Hydrophobic interaction Electrostatic interaction	Asp351, Glu419, His524 Val418, Gly420, Ile424, Leu384, Phe404, Met388, Arg394, Trp383, Glu353, Leu539 Leu525, Met421, Leu346, Leu387, Leu349, Leu391, Leu536, Leu534, Ala350
FLD-23	−9.29	154.97 nM	Hydrogen bond Hydrophobic interaction Electrostatic interaction	Met343, Asp351 Leu391, Leu428, Met388, Gly521, His524, Gly420, Phe404, Glu419, Leu354, Trp383, Thr347, Met528 Leu384, Leu387, Met421, Leu525, Ala350

tamoxifen. Specifically, FLD-5 (−13.61 kcal/mol), FLD-3 (−13.54 kcal/mol), FLD-2 (−13.15 kcal/mol), FLD-4 (−12.72 kcal/mol), and FLD-16 (−12.43 kcal/mol) showed greater affinity than quercetin (−7.50 kcal/mol) and tamoxifen (−11.40 kcal/mol). These structural modifications, particularly with benzoyl chloride

substitution, enhanced the hydrophobic interactions and binding stability within the active site of hERα. These findings are consistent with previous studies showing that flavonoid modification through alkylation or halogenation can increase binding affinity to ERα [24-25]. Furthermore, other studies have shown that flavonoid structural modification can affect binding affinity to ERα and ERβ, depending on the position and type of substituents added [25].

Hydrogen bond analysis revealed that the FLD derivatives generally formed 1–2 hydrogen bonds, with some derivatives showing none, whereas quercetin formed 2 hydrogen bonds with residues Glu353 and Glu419. Despite the relatively low number of hydrogen bonds, the FLD derivatives displayed higher binding affinity due to extensive hydrophobic interactions and electrostatic contacts. For instance, FLD-5 engaged hydrophobically with Trp383, Thr347, Met528, Gly521, His524, Gly420, Glu419, Met388, Phe404, Arg394, and Glu353, and electrostatically with Leu525, Met421, Leu393, Leu349, Leu387, Leu384, and Ala350. Other FLD derivatives similarly formed multiple hydrophobic and electrostatic interactions with key residues in the ERα binding pocket, reinforcing complex stability [25-26]. These results indicate that hydrophobic and electrostatic contributions dominate the stabilization of FLD–ERα complexes, explaining why derivatives like FLD-4 maintain strong binding and stability despite forming fewer hydrogen bonds.

The molecular docking method was validated by redocking tamoxifen into the hERα, yielding an RMSD < 2.0 Å, confirming the reliability of the docking protocol. This validation is essential before applying the method to test ligands, as a low RMSD indicates the algorithm's ability to accurately reproduce the native ligand conformation within the receptor's active site [19].

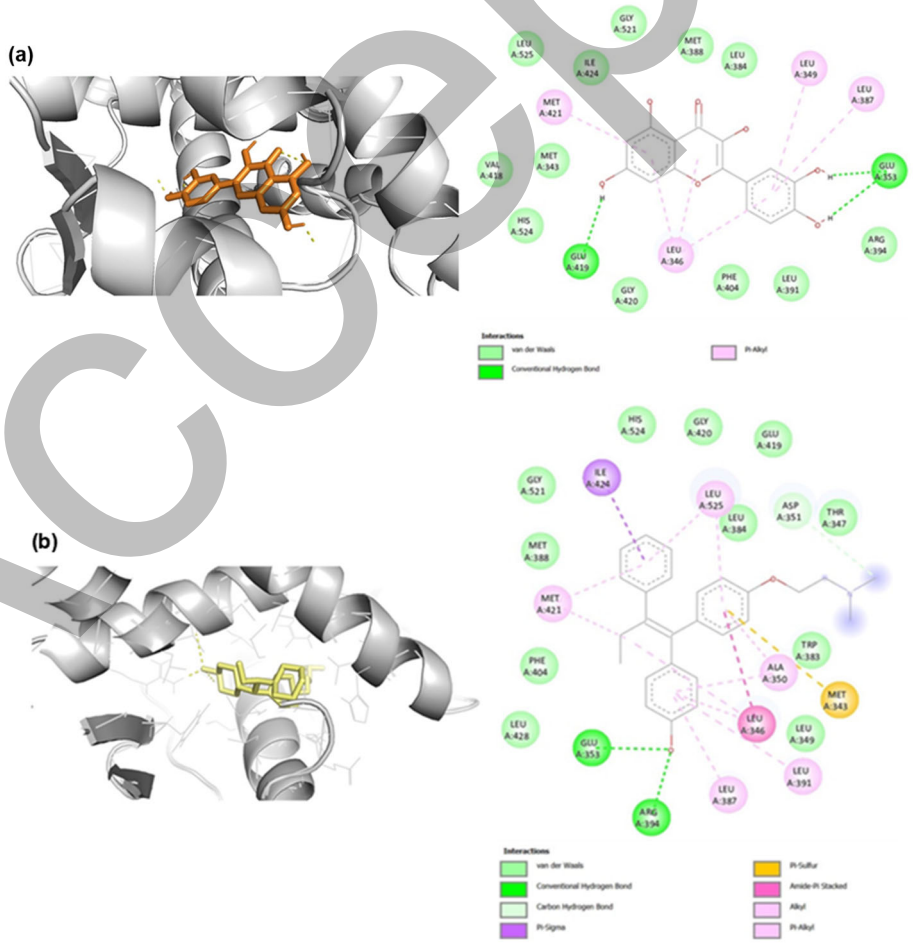

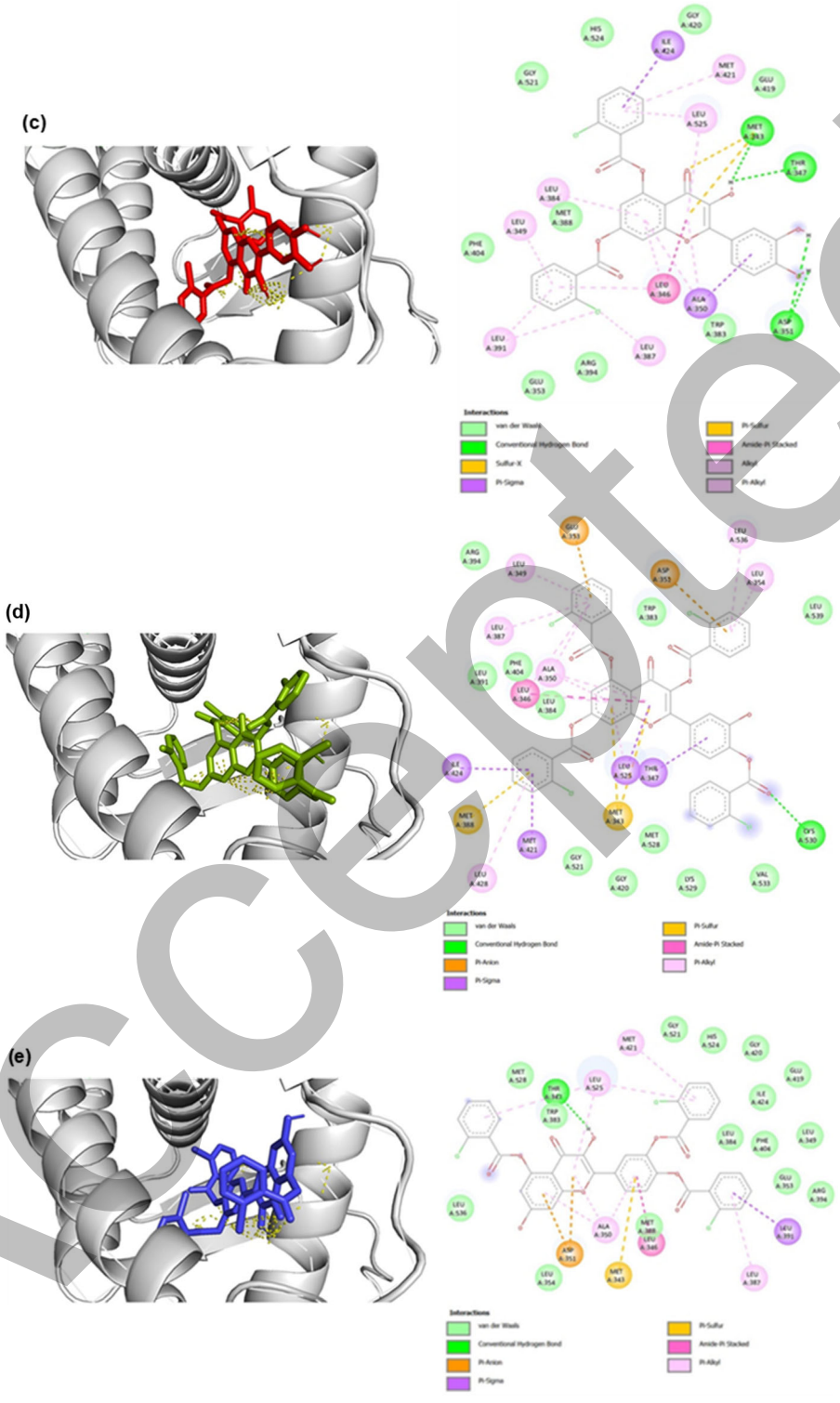

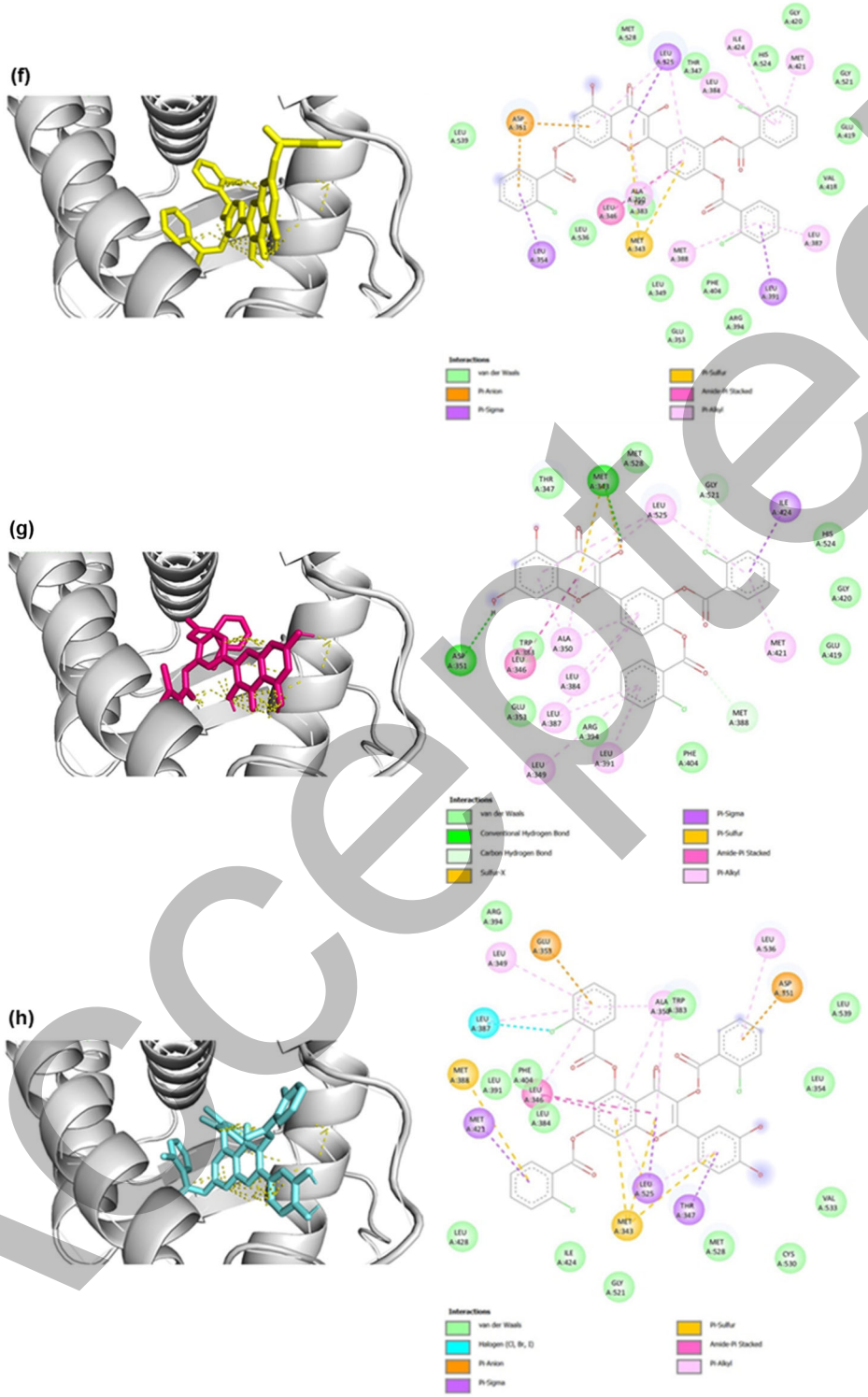

Fig 3. Molecular docking visualization results for estrogen receptor alpha (a) quercetin, (b) native ligand (tamoxifen), (c) FLD-1, (d) FLD-2, (e) FLD-3, (f) FLD-4, (g) FLD-5, and (h) FLD-6

Interestingly, the visualization of molecular interactions (Fig. 3) revealed that these top derivatives did not form hydrogen bonds with the same key residues (Glu353 and Arg394) as tamoxifen. Instead, their high affinity was

primarily supported by hydrophobic interactions (pi–pi stacking, pi-alkyl, and van der Waals contacts) within the binding pocket [20]. The introduction of chlorobenzoyl substituents in the flavonoid backbone increased aromatic surface area, thereby enhancing π-type interactions and stabilizing the ligand–receptor complex.

These findings suggest that although hydrogen bonding plays an important role in ligand stabilization, alternative non-covalent interactions can compensate for, or even surpass, its contribution to binding affinity [21]. Thus, structural modification of quercetin by chlorobenzoyl groups can generate derivatives with superior docking scores despite differences in binding mode compared to the reference drug.

ADMET Prediction

Docking of FLD series showed significant improvements compared to the parent ligand. Some derivatives, notably FLD-4 and FLD-6, exhibited lower (more negative) binding energies and smaller inhibition constants (sub-μM range), indicating enhanced binding affinity [27]. These differences can be attributed to modifications of the benzoic substituent, which strengthen hydrophobic interactions and additional hydrogen bonds with key residues in the hERα binding pocket [28]. This is consistent with structure–activity relationship (SAR) principles, where the addition of aromatic groups or electron-withdrawing substituents can increase ligand–receptor complex stability [29]. Pharmacokinetic and toxicity (ADMET) predictions showed that most quercetin derivatives have improved oral bioavailability compared to the parent compound, with polar surface area (PSA) values supporting membrane permeability [25]. Moreover, several derivatives comply with Lipinski's rule of five without significant violations and display safe toxicity profiles (non-hepatotoxic, non-mutagenic) [26]. These findings indicate that structural optimization not only enhances binding affinity but also potentially improves pharmacokinetic properties [27].

Furthermore, molecular docking visualization results demonstrate ligand interactions within the active pocket of the hERα, as shown in Fig. 4. This visualization shows the orientation of the modified compounds within the receptor's active pocket, along with the amino acid residues that form non-covalent interactions, such as hydrogen bonds and hydrophobic interactions, which enhance ligand affinity for the receptor. *In silico* pharmacokinetic and toxicological properties of FLD-derived compounds were predicted using the pkCSM server, including absorption, distribution, metabolism, excretion, and toxicity parameters.

In terms of absorption parameters, almost all FLD-derived compounds exhibited high human intestinal absorption (HIA) values (> 90%), with good to moderate water solubility. Two compounds, FLD-7 and FLD-11, fell into the moderate category with HIA < 90%. Regarding distribution, most compounds had moderate volume of distribution (VDss) values, indicating adequate tissue distribution. Several compounds, particularly FLD-2, FLD-5, and FLD-22, are predicted to cross the blood-brain barrier (BBB+), while others are BBB–. Metabolism prediction results show that almost all compounds are substrates of the CYP3A4 enzyme, with certain compounds (FLD-10, FLD-12, FLD-18, and FLD-20) also having the potential to act as inhibitors. Meanwhile, interactions with CYP2D6 are relatively insignificant.

In terms of excretion, total clearance values vary among compounds: FLD-1, FLD-3, and FLD-5 have relatively faster elimination rates, while FLD-16 and FLD-22 are slower, which may affect their half-lives in the body. Regarding toxicity, most FLD compounds are predicted to be safe, with negative Ames test results (non-mutagenic) and low hepatotoxicity potential. However, FLD-7 and FLD-17 exhibited potential moderate hepatotoxicity and

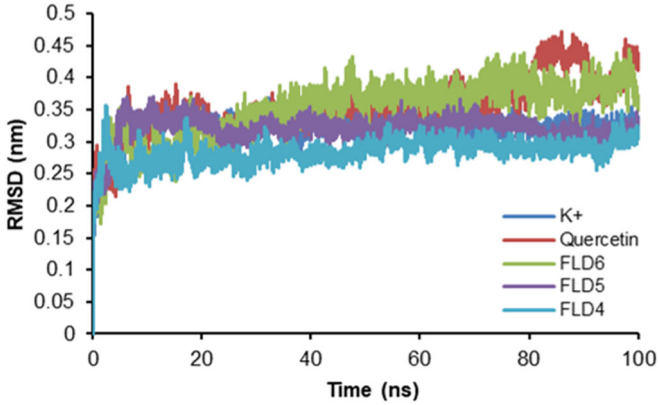

Fig 4. RMSD results of MD simulation

require special attention in further evaluation. No compounds were found to be cardiotoxic via hERG channel inhibition. Overall, the ADMET profiles of FLD compounds indicate that most have good prospects for development as drug candidates, with high bioavailability, adequate tissue penetration, and low toxicity. A summary of the ADMET prediction results is presented in Table 4.

Several benzoylated quercetin derivatives, particularly FLD-6, exhibited molecular weights exceeding 900 Da, which places them outside the optimal drug-like space according to Lipinski's Rule of Five. Such large molecules often exhibit poor ADME properties, making them less suitable as oral drug candidates. However, these highly substituted derivatives could still retain pharmacological relevance through prodrug or soft-drug strategies, in which the compound either releases the active quercetin scaffold after enzymatic activation or undergoes controlled metabolic inactivation to enhance safety and reduce systemic exposure. Future optimization should thus focus on derivatives within a molecular weight range of 300–600 Da to balance lipophilicity, stability, and bioavailability, ensuring improved compliance with modern drug-likeness criteria.

Table 4. ADMET of quercetin compounds and their derivatives

No	Compound	Absorption			Distribution		
		Water solubility (log mol/L)	Caco-2 permeability (log Papp, 10^{-6} cm/s)	Intestinal absorption (%absorbed)	VDss (log L/kg)	BBB permeability (log BB)	CNS permeability (log PS)
1	Quercetin	−3.24	0.587	74.99	0.14	Non-penetrable (High confidence)	3.12
2	FLD-1	−3.524	0.180	100	−1.793	−1.775	−3.305
3	FLD-2	−2.905	−0.276	100	−1.077	−2.256	−3.043
4	FLD-3	−3.105	0.252	100	−1.677	−0.985	−3.005
5	FLD-4	−3.781	0.109	89.46	−1.727	−1.964	−3.117
6	FLD-5	−3.123	0.162	100	−1.673	−1.090	−3.084
7	FLD-6	−2.892	−0.322	100	−0.042	−2.941	−2.910
8	FLD-7	−3.357	0.102	83.80	−0.756	−1.596	−3.417
9	FLD-8	−3.075	−0.332	100	−1.692	−1.886	−3.239
10	FLD-9	−2.902	−0.277	100	−0.986	−2.397	−2.954
11	FLD-10	−3.720	0.254	95.10	−1.685	−1.604	−3.122
12	FLD-11	−3.301	0.191	86.39	−0.758	−1.404	−3.338
13	FLD-12	−3.461	0.063	99.22	−1.647	−1.777	−3.283
14	FLD-13	−3.545	0.282	93.07	−1.701	−1.643	−3.142
15	FLD-14	−3.075	−0.231	100	−1.629	1.714	−3.087
16	FLD-15	−3.551	−0.343	91.54	−1.620	−1.837	−3.171
17	FLD-16	−3.087	−0.389	100	−1.538	−1.237	−3.038
18	FLD-17	−3.781	0.109	89.46	−1.727	−1.964	−3.117
19	FLD-18	−3.407	0.139	75.54	−0.791	−1.614	−3.254
20	FLD-19	−2.912	0.613	88.75	−0.836	−1.901	−3.351
21	FLD-20	−3.816	0.164	92.52	−1.673	−1.813	−3.200
22	FLD-21	−3.511	−0.344	99.80	−1.638	−1.830	−3.332
23	FLD-22	−3.369	−0.084	84.80	−0.862	−1.582	−3.367
24	FLD-23	−3.728	−0.004	93.52	−1.604	−1.823	−3.155

No	Compound	Metabolism				Excretion		Toxicity	
		CYP2D6	CYP3A4	CYP1A2	CYP2C9	Total clearance (log mL/min/kg)	Renal OCT2	AMES toxicity	Hepatotoxicity
1	Quercetin	Yes	Yes	Yes	No	−8.91	No	No	Yes
2	FLD-1	No	Yes	No	Yes	−0.035	No	No	Yes
3	FLD-2	No	Yes	No	No	−0.111	No	No	No
4	FLD-3	No	Yes	No	Yes	−0.075	No	No	No

No	Compound	Metabolism				Excretion		Toxicity	
		CYP2D6	CYP3A4	CYP1A2	CYP2C9	Total clearance (log mL/min/kg)	Renal OCT2	AMES toxicity	Hepatotoxicity
5	FLD-4	No	Yes	No	Yes	−0.041	No	No	Yes
6	FLD-5	No	Yes	No	Yes	−0.080	No	No	No
7	FLD-6	No	Yes	No	No	−0.128	No	No	No
8	FLD-7	No	Yes	No	Yes	0.002	No	No	Yes
9	FLD-8	No	Yes	No	Yes	−0.073	No	No	No
10	FLD-9	No	Yes	No	No	−0.105	No	No	No
11	FLD-10	No	Yes	No	Yes	−0.041	No	No	Yes
12	FLD-11	No	Yes	No	Yes	0.009	No	No	No
13	FLD-12	No	Yes	No	Yes	−0.038	No	No	Yes
14	FLD-13	No	Yes	No	Yes	−0.050	No	No	Yes
15	FLD-14	No	Yes	No	Yes	−0.084	No	No	No
16	FLD-15	No	Yes	No	Yes	−0.052	No	No	Yes
17	FLD-16	No	Yes	No	Yes	−0.078	No	No	No
18	FLD-17	No	Yes	No	Yes	−0.041	No	No	Yes
19	FLD-18	No	Yes	No	Yes	−0.008	No	No	Yes
20	FLD-19	No	Yes	No	Yes	−0.039	No	No	Yes
21	FLD-20	No	Yes	No	Yes	−0.047	No	No	Yes
22	FLD-21	No	Yes	No	Yes	−0.044	No	No	Yes
23	FLD-22	No	Yes	No	Yes	0.008	No	No	Yes
24	FLD-23	No	Yes	No	Yes	−0.042	No	No	Yes

MD Simulations and MMP-BSA

MD simulations for 100 ns showed that the protein-ligand complex reached stability after an equilibration phase of 10–15 ns. RMSD analysis showed that the quercetin derivative FLD-4 had the highest stability, with an average deviation of approximately 0.30 nm, which remained relatively flat throughout the simulation, while FLD-6 exhibited the largest fluctuations, approaching 0.45 nm (Fig. 4). SASA results supported these findings, as FLD-4 and the control (K+) maintained lower solubilized surface areas (131–133 nm^2), indicating a more compact complex structure than the parent quercetin and FLD-6 (Fig. 5).

Further RMSF analysis indicates that the protein core remains stable, with low fluctuations (< 0.3 nm), while striking differences emerge at the termini. Complexes with FLD-4 and FLD-5 suppress the movement of the terminal residues (0.6–0.9 nm) compared to the parent quercetin and FLD-6, which reach > 1.0 nm. Overall, the combination of these three parameters suggests that FLD-4 is the most promising candidate, producing a stable, compact complex with more controlled flexibility of the terminal residues (Fig. 6) [29].

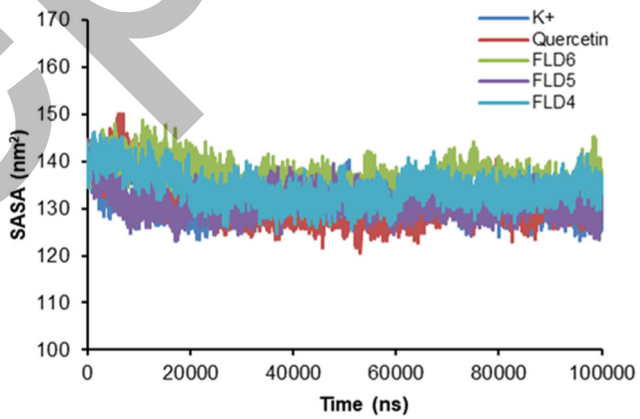

Fig 5. SASA of hERα with ligand

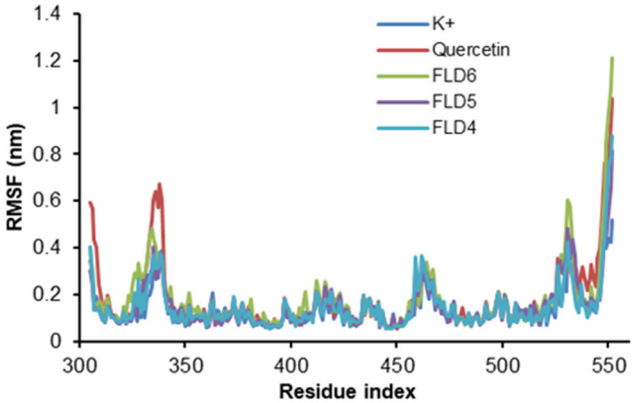

Fig 6. RMSF of hERα with ligand

Table 5. Results of MMP-BSA analysis in kJ/mol

Compound	ΔE_vdw	ΔE_elec	ΔG_polar	ΔG_nonpolar	ΔG_bind	Stability
Quercetin	−120.947 ± 13.486	−192.203 ± 8.209	−67.163 ± 14.502	188.244 ± 23.648	−49.826 ± 1.304	Moderately stable
Drug compound	−199.309 ± 16.271	−230.761 ± 5.023	−51.884 ± 19.172	129.467 ± 26.919	−23.407 ± 0.781	Stable
FLD-5	−177.003 ± 18.152	−284.697 ± 14.778	−37.085 ± 20.654	171.095 ± 27.649	−26.316 ± 1.030	Stable
FLD-6	−183.970 ± 27.471	−268.498 ± 12.290	−36.648 ± 25.827	147.632 ± 30.123	−26.456 ± 1.311	Very stable
FLD-4	−205.409 ± 17.844	−316.037 ± 18.940	−47.630 ± 11.106	189.031 ± 16.767	−30.773 ± 1.012	Most stable (best)

MMP-BSA analysis strengthens these results with the calculation of decomposed free binding energy. Quercetin shows a total binding energy of −120.947 ± 13.486 kJ/mol, lower than the reference drug compound (−199.309 ± 16.271 kJ/mol). FLD derivatives show increased affinity, especially FLD-4 with a value of −205.409 ± 17.844 kJ/mol and the strongest van der Waals energy contribution (−316.037 ± 18.940 kJ/mol), thus interpreted as the most stable and best complex among all tested ligands shown in Table 5. These results are consistent with the structural stability indicated by RMSD, RMSF, and SASA analysis.

MM-PBSA analysis confirmed the docking results by showing that the FLD-4 complex had the lowest total binding energy (−205.409 ± 17.844 kJ/mol) compared to quercetin (−120.947 ± 13.486 kJ/mol), tamoxifen (−199.309 ± 16.271 kJ/mol), and other derivatives. The increased binding affinity of FLD-4 was mainly due to stronger electrostatic and van der Waals interactions. These results were consistent with MD simulation data, which showed the stability of the FLD-4 structure, with low RMSD fluctuations and minimal SASA. These findings support the hypothesis that structural modification of quercetin, specifically by substitution of benzoyl chloride at positions 3, 5, and 7 (ring A), and 3′ and 4′ (ring B), can increase complex stability and binding affinity to hERα. Previous studies have also shown that flavonoid modification via alkylation or halogenation can increase complex stability and binding affinity to ERα.

■ CONCLUSION

This study demonstrated that structural modification of quercetin, particularly in the FLD-4 derivative, significantly improved its binding affinity, structural stability, and pharmacokinetic properties compared with native quercetin. Computational analyses, including molecular docking, ADMET prediction, molecular dynamics simulation, and MM-PBSA, consistently highlighted FLD-4 as the most promising candidate targeting ERα in breast cancer. These findings provide a solid foundation for subsequent in vitro and in vivo studies to validate and advance FLD-4 toward preclinical evaluation.

■ ACKNOWLEDGMENTS

This study was supported by a Regular Fundamental Research Grant, chaired by Dwi Utami from the Directorate of Research and Community Service, Directorate General of Research and Development, Ministry of Higher Education, Science and Technology Service for the fiscal year 2025, number 039/PFR/LPPM.UAD/VI/2025, dated June 5, 2025. Special thanks are also extended to the Doctoral Program of Pharmaceutical Sciences, Faculty of Pharmacy, Universitas Ahmad Dahlan, and the Faculty of Pharmacy, Universitas Islam Kalimantan MAB Banjarmasin, for their academic and technical support throughout this study.

■ CONFLICT OF INTEREST

The authors declare that they have no conflicts of interest regarding this research.

■ AUTHOR CONTRIBUTIONS

Dwi Utami and Muhammad Fauzi conceptualized the study. Laela Hayu Nurani and Any Guntarti supervised the research design and methodology. Citra Ariani Edityaningrum, Mustofa Ahda, and Sugiyanto performed molecular docking and ADMET analyses. Lalu Muhammad Irham carried out molecular dynamics simulations and data validation. Fara Azzahra and Arif Budi Setianto assisted in data curation and visualization.

Dwi Utami, Muhammad Fauzi, and Laela Hayu Nurani wrote the initial draft. All authors contributed to the review, editing, and approval of the final version of the manuscript.

■ REFERENCES

[1] Ferlay, J., Colombet, M., Soerjomataram, I., Parkin, D.M., Piñeros, M., Znaor, A., and Bray, F., 2021, Cancer statistics for the year 2020: An overview, *Int. J. Cancer*, 149 (4), 778–789.

[2] Bray, F., Laversanne, M., Sung, H., Ferlay, J., Siegel, R.L., Soerjomataram, I., and Jemal, A., 2024, Global cancer statistics 2022: GLOBOCAN estimates of incidence and mortality worldwide for 36 cancers in 185 countries, *CA: Cancer J. Clin.*, 74 (3), 229–263.

[3] Osborne, A., Adnani, Q.E.S., and Ahinkorah, B.O., 2025, Breast cancer incidence in Indonesia: A sex-disaggregated analysis using WHO health equity assessment toolkit data, *BMC Cancer*, 25 (1), 986.

[4] Wu, Z.Y., Qiu, K.Y., Gai, Y.J., Wu, J.H., Zhou, B.X., and Shi, Q.F., 2025, Quercetin: A natural ally in combating breast cancer, *Int. J. Nanomed.*, 20, 9155–9177.

[5] Frenț, O.D., Stefan, L., Morgovan, C.M., Duteanu, N., Dejeu, I.L., Marian, E., Vicaș, L., and Manole, F., 2024, A systematic review: Quercetin—secondary metabolite of the flavonol class, with multiple health benefits and low bioavailability, *Int. J. Mol. Sci.*, 25 (22), 12091.

[6] Alizadeh, S.R., and Ebrahimzadeh, M.A., 2022, *O*-substituted quercetin derivatives: Structural classification, drug design, development, and biological activities, A review, *J. Mol. Struct.*, 1254, 132392.

[7] Khater, M., Watson, K.A., Boateng, S.Y., Greco, F., and Osborn, H.M.I., 2022, Halogenated flavonoid derivatives display antiangiogenic activity, *Molecules*, 27 (15), 4757.

[8] Fauzi, M., Nurani, L.H., Utami, D., And Irham, L.M., 2025, Quercetin: Synthesis trends, chemical reactions, and its role as an estrogen receptor alpha modulator in breast cancer therapy: A systematic literature review, *Trends Sci.*, 22 (8), 9423.

[9] Ahda, M., Ahmed, Q.U., Utami, D., Mahfudh, N., Syahputra, R., Anwar, M., Hernawan, H., Hanifah, D., Fithri, H.H.Z., Bin Abdul Hamid, A.A., Rofiee, M.S., Jaswir, I., Khatib, A., and Uddin, A.H., 2025, *Orthosiphon aristatus* leaf extracts as α-glucosidase and soybean lipoxygenase inhibitors and their toxicity: *In-vitro* and *in-silico* approaches, *Rev. Bras. Farmacogn.*, 35 (6), 1468–1482.

[10] Roney, M., and Mohd Aluwi, M.F.F., 2024, The importance of *in-silico* studies in drug discovery, *Intell. Pharm.*, 2 (4), 578–579.

[11] Ayoub, N., Pietrancosta, N., Gianetto, Q.G., Karimova, G., Gedeon, A., and Munier-Lehmann, H., 2026, Exploring the multi-protein assembly of the enzymes of the *de novo* purine nucleotide biosynthetic pathway from *Pseudomonas aeruginosa*, *Int. J. Biol. Macromol.*, 343, 149706.

[12] Schrödinger LLC, 2015, *The Pymol Molecular Graphics System*, Version 1.8.

[13] Daina, A., Michielin, O., and Zoete, V., 2017, SwissADME: A free web tool to evaluate pharmacokinetics, drug-likeness and medicinal chemistry friendliness of small molecules, *Sci. Rep.*, 7 (1), 42717.

[14] Abraham, M.J., Murtola, T., Schulz, R., Páll, S., Smith, J.C., Hess, B., and Lindahl, E., 2015, GROMACS: High performance molecular simulations through multi-level parallelism from laptops to supercomputers, *SoftwareX*, 1-2, 19–25.

[15] Latifa, N., Rais, I.R., Prasasti, D., and Utami, D., 2024, Potential cervical anticancer activity of tomcat beetle (*Paederus fuscipes*) compounds against estrogen alpha receptor (3ert): In silico study, *BIO Web Conf.*, 148, 04013.

[16] Essa, A.F., Teleb, M., El-Kersh, D.M., El Gendy, A.E.N.G., Elshamy, A.I., and Farag, M.A., 2023, Natural acylated flavonoids: Their chemistry and biological merits in context to molecular docking studies, *Phytochem. Rev.*, 22 (6), 1469–1508.

[17] Terefe, E.M., and Ghosh, A., 2022, Molecular docking, validation, dynamics simulations, and pharmacokinetic prediction of phytochemicals isolated from *Croton dichogamus* against the HIV-

1 reverse transcriptase, *Bioinf. Biol. Insights*, 16, 11779322221125604.

[18] Lo, S., Leung, E., Fedrizzi, B., and Barker, D., 2021, Synthesis, antiproliferative activity and radical scavenging ability of 5-*O*-acyl derivatives of quercetin, *Molecules*, 26 (6), 1608.

[19] Yeni, Y., and Rachmania, R.A., 2022, The prediction of pharmacokinetic properties of compounds in *Hemigraphis alternata* (Burm.F.) T. Ander leaves using pkCSM, *Indones. J. Chem.*, 22 (4), 1081–1089.

[20] Asghar, S., Hameed, S., Al-Masoudi, N.A., Saeed, B., and Shtaiwi, A., 2024, Design, synthesis, docking studies and molecular dynamics simulation of new 1,3,5-triazine derivatives as anticancer agents selectively targeting pancreatic adenocarcinoma (Capan-1), *Chem. Biodiversity*, 21 (5), e202400112.

[21] Nurisyah, N., Ramadhan, D.S.F., Dewi, R., Asikin, A., Daswi, D.R., Adam, A., Chaerunnimah, C., Sunarto, S., Rafika, R., Artati, A., and Fakih, T.M., 2024, Targeting EGFR allosteric site with marine-natural products of *Clathria* sp.: A computational approach, *Curr. Res. Struct. Biol.*, 7, 100125.

[22] Rajesh, G.D., Apte, K., Abhirami, P.V., Anusha, S., Ranjitha, A., Kumar, S.B., Sarvottam, K., and Kumar, P., 2025, Comprehensive *in silico* analysis of flavonoids in breast cancer using molecular docking, ADME, and molecular dynamics simulation approach, *Pept. Sci.*, 117 (1), E24391.

[23] Wang, W., Sun, C., Mao, L., Ma, P., Liu, F., Yang, J., and Gao, Y., 2016, The biological activities, chemical stability, metabolism and delivery systems of quercetin: A review, *Trends Food Sci. Technol.*, 56, 21–38.

[24] Sim, J., Kim, D., Kim, B., Choi, J., and Lee, J., 2025, Recent advances in AI-driven protein–ligand interaction predictions, *Curr. Opin. Struct. Biol.*, 80, 102589.

[25] Safna Hussan, K.P., Davis, A., Lekshmi, S., Shahin Thayyil, M., Chathrattil Raghavamenon, A., and Devassy Babu, T., 2024, Evaluation of the binding efficacy of flavonol derivatives on estrogen receptors (ER) with respect to ring B hydroxylation, *Results Chem.*, 7, 101544.

[26] Lee, S., and Barron, M.G., 2017, Structure-based understanding of binding affinity and mode of estrogen receptor α agonists and antagonists, *PloS One*, 12 (1), E0169607

[27] Sultan, R., Ahmed, A., Wei, L., Saeed, H., Islam, M., and Ishaq, M., 2023, The anticancer potential of chemical constituents of *Moringa oleifera* targeting CDK-2 inhibition in estrogen receptor positive breast cancer using *in-silico* and *in vitro* approches, *BMC Complement. Med. Ther.*, 23 (1), 396.

[28] Shaw, S., Chourasia, M., Nayak, R., Kumeria, T., Ghosh, M.P., Santoshi, S., and Bose, S., 2025, Molecular interaction of quercetin and its derivatives against nucleolin in breast cancer: *In-silico* and *in-vitro* study, *J. Biomol. Struct. Dyn.*, 43 (14), 7348–7359.

[29] Parihar, A., Puranik, N., Nadda, A.K., Kumar, V., Lee, K.W., Kumar, R., Khandia, R., And Khan, R., 2024, Phytochemicals for breast cancer therapeutic intervention: Exploratory *in silico* molecular docking study, *Medinformatics*, 0 (0), 1–15.